Ionics (2016) 22:1003–1009
DOI 10.1007/s11581-016-1639-8

ORIGINAL PAPER

Synthesis and electrochemical performance of spherical $LiNi_{0.8}Co_{0.15}Ti_{0.05}O_2$ cathode materials with high tap density

Mingwu Xiang[1] · **Wei Tao**[1] · **Jinhua Wu**[1,2] · **Yan Wang**[3] · **Heng Liu**[1]

Received: 8 September 2015 / Revised: 16 December 2015 / Accepted: 2 January 2016 / Published online: 23 January 2016

Abstract A series of spherical $LiNi_{0.8}Co_{0.15}Ti_{0.05}O_2$ cathode materials were synthesized through co-oxidation-controlled crystallization method followed by solid-state reaction at different calcination temperatures under oxygen flowing. The crystal structure and particles morphology of the as-prepared powders were characterized by X-ray diffraction (XRD) and scanning electron microscopy (SEM), respectively. All samples correspond to the layered α-$NaFeO_2$ structure with R-3m space group. The $LiNi_{0.8}Co_{0.15}Ti_{0.05}O_2$ prepared at 800 °C presents a better hexagonal ordering structure and better spherical particles and possesses a high tap density of 3.22 g cm^{-3}. Meanwhile, the NCT-2 sample exhibits an advanced electrochemical performance with an initial discharge capacity of 174.2 mAh g^{-1} and capacity retention of 86.7 % after 30 cycles at 0.2 C.

Keywords Lithium-ion battery · Cathode material · $LiNi_{0.8}Co_{0.15}Ti_{0.05}O_2$ · Solid-state reaction · High tap density

Introduction

With the increasing development of the portable electronic devices, electric vehicles (EVs) and hybrid electrical vehicles (HEVs), it is necessary to break the bottleneck of high capacity density, long cycle life, good security, and excellent rate capability for lithium-ion batteries [1–3]. Nickel-rich layered $Li(Ni_xM_{1-x})O_2$ cathode materials with high discharge specific capacity, great rate capability and relatively low cost are becoming one of the most promising cathode materials for lithium-ion battery. On the basis of Co-doped $LiNiO_2$, it has been proven that the addition of an extra element (such as Al, Ti, Mn, Mg, Fe, Y, and Sr) may effectively improve the thermostability and cycling stability of $LiNi_{0.8}Co_{0.2}O_2$ electrode material [4–7]. For example, as the isomorphous solid solution of $LiNiO_2$, $LiCoO_2$, and $LiAlO_2$, $LiNi_{0.8}Co_{0.15}Al_{0.05}O_2$ with a high tap density, an excellent rate capability and cycling stability is considered to be the next generation cathode materials for green lithium-ion battery [8].

Nickel-rich layered cathode materials have been developed in the direction of high tap density with the increasing requirements of high volume capacity density. Among the doping elements, an appropriate amount of Ti doping in Nickel-rich layered materials can enhance structural integrity and thermostability because the Ti^{4+} ions prevent impurity Ni^{2+} migration into the lithium sites [9–11]. Hongwei Tang et al. [12] had successfully prepared $LiNi_{0.8}Co_{0.15}Ti_{0.05}O_2$ powders with a high tap density of 3.17 g cm^{-3}. However, the $LiNi_{0.8}Co_{0.15}Ti_{0.05}O_2$ powders are smooth-edged polyhedrals and their average sizes are 3 ~ 5 μm. It is well known that the as-prepared particles with spherical morphology are more conducive to enhancing the dense packing of materials and improving the tap density. In addition, spherical particles are advantageous to facilitate the infiltration between the electrolyte and active materials and also can effectively shorten the lithium-ion diffusion channels.

In this paper, the $LiNi_{0.8}Co_{0.15}Ti_{0.05}O_2$ cathode materials with a good spherical morphology and a high

✉ Heng Liu
h_liu@scu.edu.cn

[1] College of Materials Science and Engineering, Sichuan University, Chengdu 610064, People's Republic of China

[2] Department of Materials Engineering, Sichuan College of Architectural Technology, Deyang 618000, People's Republic of China

[3] College of Computer Science and Technology, Southwest University for Nationalities, Chengdu 610041, People's Republic of China

tap density have been prepared successfully by using the spherical $Ni_{0.8}Co_{0.15}(OH)_{1.9}$ as precursor which was synthesized via a co-oxidation-controlled crystallization method. The effects of calcination temperature on the crystalline structure, micromorphology, and electrochemical performance of the titanium substitutive $LiNi_{0.8}Co_{0.15}Ti_{0.05}O_2$ cathode materials were further investigated.

Experimental section

Sample preparation

The $Ni_{0.8}Co_{0.15}(OH)_{1.9}$ precursor was obtained by the co-oxidation-controlled crystallization method described in our previous report [13]. The mixing metal ion solution of Ni and Co according to the stoichiometric of n(Ni):n(Co) = 0.8:0.15 was prepared by dissolving $NiSO_4{\cdot}6H_2O$ and $CoSO_4{\cdot}7H_2O$ in deionized water. The metallic ion solution was made into 2 mol/L, while the NaOH solution was 4 mol/L. Commercial ammonia solution (28 wt %, as the chelating agent) was added to the NaOH solution to maintain a NH_3/NH_4OH molar ratio (≈0.54). The metallic ion solution and the NaOH solution were added into the four-neck flask reactor through the charging ports, respectively, while the other one was connected to a pH sensor/controller. The as-prepared precursor of 0.8 g as a crystal nucleus was added into 100 mL deionized water before the reaction. The pumping rate of both the metallic ion solution and the NaOH solution was automatically controlled by a peristaltic pump (Leadfluid, China), and the injection rate was kept at 0.15 mL/min to maintain a constant pH of 11.0 ± 0.1. And then, the reaction solution was stirred continuously with a speed of 1000 rpm and the water bath temperature was controlled at 60 °C. The product slurry was aged about 5 h, washed, and then dried at 120 °C. The obtained precursor was ground with an excess of $LiOH{\bullet}H_2O$ (Li/(Ni + Co + Ti) = 1.01) and a stoichiometry of TiO_2. The mixture was calcined at different temperatures (750, 800, and 850 °C) for 16 h in oxygen flowing atmosphere. Finally, three $LiNi_{0.8}Co_{0.15}Ti_{0.05}O_2$ powders were obtained, which were correspondently marked as NCT-1, NCT-2, and NCT-3 samples.

Characterization

Powder X-ray diffraction (XRD, Philips X'pert TRO MPD, Germany) using Cu Kα radiation at 40 kV/25 mA and at 0.06° s^{-1} was employed to characterize the crystal phase of the samples. The particle morphology and particle size of the samples were observed by scanning electron microscopy (SEM; JSM-5900LV, Japan).

Electrochemical measurements

The electrochemical characteristics of the synthesized cathode materials were carried out using a two-electrode test cell with lithium foil as the negative electrode. A positive electrode was made by coating the slurry mixture composed of $LiNi_{0.8}Co_{0.15}Ti_{0.05}O_2$ active material, Super P, and polyvinylidene fluoride (PVDF) binder (in the weight ratio of 86:7:7) on an aluminum-foil collector, with nmethylpyrrolidone (NMP) as the solvent. The positive film was subjected to roll press and the electrodes of 14 mm diameter were punched out. The positive electrodes were dried at 120 °C for 12 h in a vacuum oven. The coin-type cells (CR2032) were assembled in a glove box filled Argon with an electrolyte of 1 mol L^{-1} $LiPF_6$ in EC-DMC-EMC (1:1:1, volume ratio) solution. Charge/discharge performance of the cells was investigated using a Neware BTS-610 Tester (Neware BTS-610, China) between 2.5 and 4.5 V at different rates (1 C = 170 mAh g^{-1}) at 30 °C. Cyclic voltammogram (CV) was measured on a LK9805 electrochemical interface at a scanning rate of 0.1 mV s^{-1}.

Results and discussion

Structural analysis

Figure 1 shows the XRD patterns of NCT-1, NCT-2, and NCT-3 samples. All diffraction peaks of three samples can be indexed to single phase of hexagonal α-$NaFeO_2$ structure with a space group of R-3m, and no new peaks corresponding to impurity phase TiO_2 or other titanium oxides were detected. The previous work has demonstrated that clear splitting of the (006)/(102) and (108)/(110) peaks indicates a high degree of ordered layered structure [14, 15]. The overlapped (006)/(102) and (018)/(110) characteristic peaks were discovered in

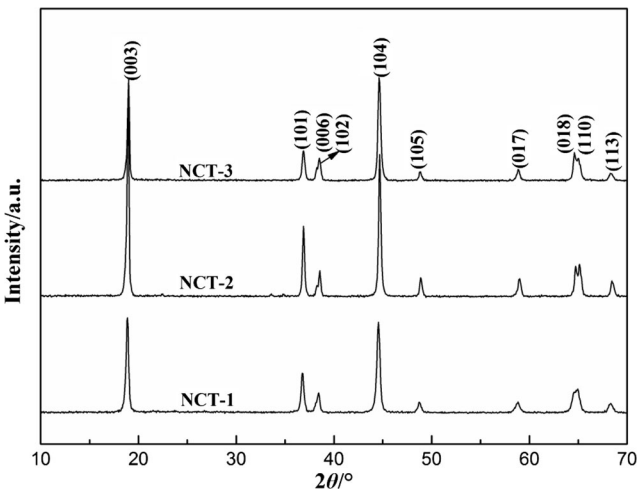

Fig. 1 The XRD patterns of NCT-1, NCT-2, and NCT-3 samples

NCT-1 and NCT-3 samples; however, the (018)/(110) peaks were well separated in NCT-2 sample. This result suggests that the NCT-2 sample possesses a better hexagonal ordering structure [16]. Compared with NCT-1 and NCT-3 samples, the NCT-2 sample shows more sharp diffraction peaks and stronger peaks intensity, indicating an improved crystallinity.

The lattice parameters were calculated according to XRD data using Jade 6.0 as shown in Table 1. Higher values of c/a ratios are acknowledged as a less degree of cation mixing [17–20]. In addition, the $I(003)/I(104)$ ratio also has been used as a degree of cation mixing, that is, the values lower than 1.2 indicate a high degree of cation mixing, due to other metal ions occupy the lithium site and the reversible capacity of the cathode material tends to decrease when the $I(003)/I(104)$ ratio is less than 1.2 [21–24]. The presence of disorder on the Li site is closely associated with the calcination temperatures [25]. According to the XRD result, the NCT-2 sample shows a higher value of c/a and $I(003)/I(104)$ ratios, indicating the lowest degree of cation mixing. On the contrary, that of the NCT-1 and NCT-3 samples clearly shows a smaller value. This demonstrates that temperatures below 800 °C are insufficient to promote full site ordering, namely indication of severe cation mixing. However, if the temperature is too high, nonstoichiometry and disorder on the Li site will also be introduced due to the part volatilization of lithium [26, 27]. These results suggest that the calcination temperature can effectively affect the crystalline structure of $LiNi_{0.8}Co_{0.15}Ti_{0.05}O_2$ cathode materials during the synthesis process.

Morphological characterization

Figure 2 shows SEM images of the $Ni_{0.8}Co_{0.15}(OH)_{1.9}$ precursor and all the $LiNi_{0.8}Co_{0.15}Ti_{0.05}O_2$ powders. As shown in Fig. 2 (A and A′), the secondary particles consisted of the dense agglomeration of needle-like shape primary particles. The precursor had spherical morphology and its particle size and tap density were 2 ~ 3 μm in diameter and 1.91 g cm^{-3}, respectively. It can be discovered that all the $LiNi_{0.8}Co_{0.15}Ti_{0.05}O_2$ samples inherited the spherical morphology of the precursor, as shown in Fig. 2 (B and B′), (C and C′), and (D and D’). The spherical particles were advantageous to facilitate the infiltration between the electrolyte and active materials and effectively shorten the lithium-ion diffusion channels in the intercalation/deintercalation process. Compared with the needle-shaped primary particles morphology of precursor, the $LiNi_{0.8}Co_{0.15}Ti_{0.05}O_2$ particles size increases with the increase of calcination temperature. Moreover, the NCT-1, NCT-2, and NCT-3 samples show a high tap density of 3.02, 3.22, and 3.23 g cm^{-3}, respectively. Because the spherical particles have fewer interspace in particles interface. The $LiNi_{0.8}Co_{0.15}Ti_{0.05}O_2$ cathode materials with a high tap density can enhance its volumetric energy and advance the applications in large scale energy supplies.

Table 1 The cell parameters of NCT-1, NCT-2, and NCT-3 samples

Sample	a (±0.0001 Å)	c (±0.0008 Å)	c/a	$I_{(003)}/I_{(104)}$
NCT-1	2.868	14.148	4.93	1.05
NCT-2	2.861	14.143	4.94	1.43
NCT-3	2.864	14.145	4.94	0.98

EDS analysis

Figure 3 presents the SEM (A) and EDS images (B) of the NCT-2 sample. The composition of NCT-2 sample was examined by EDS and the element percentage was presented in Table 2. The result shows that the atomic percentage of Ni:Co:Ti approximates the ratio of 80:15:4.5, which indicates the effective incorporation of titanium in the particles and the co-oxidation-controlled crystallization combine with solid-state reaction can synthesis spherical and stoichiometric $LiNi_{0.8}Co_{0.15}Ti_{0.05}O_2$ cathode materials with homogeneous Ti element distribution.

Electrochemical properties

Figure 4 presents the rate and cycling performance curves of NCT-1, NCT-2, and NCT-3 samples at different rates from 0.05 to 5 C. As shown in Fig. 4a, the NCT-2 sample shows a better electrochemical performance at low rate (from 0.05 to 1.0 C). With the rate increase from 1 to 5 C, electrochemical properties of all the samples suddenly reduced. Figure 4b displays the cycling performance curves of all $LiNi_{0.8}Co_{0.15}Ti_{0.05}O_2$ cathode materials at 0.2 C. The initial discharge specific capacity of NCT-1, NCT-2, and NCT-3 samples were 161.2, 174.2, and 166.3 mAh g^{-1}, respectively. And the NCT-1, NCT-2, and NCT-3 samples reveal the capacity retentions of 80.0, 86.7, and 86.5 % after 30 cycles, respectively. Figure 4c shows the coulomb efficiencies of all samples at different rate from 0.05 to 5 C, while their initial coulomb efficiencies are about 85 % at lower 0.05 C. Afterwards, all samples show an excellent coulomb efficiency of approximate 99 %. The typical initial charge/discharge curves of NCT-1, NCT-2, and NCT-3 samples in the voltage range of 2.5–4.5 V at 0.2 C are shown in Fig. 4d. A clear and constant potential plateau near 3.8 V was very similar to the three samples. However, the NCT-2 obviously exhibits a longer discharge plateau and releases a higher initial discharge specific capacity of 174.2 mAh g^{-1} than NCT-1 and NCT-3. These results indicated that calcination temperature has

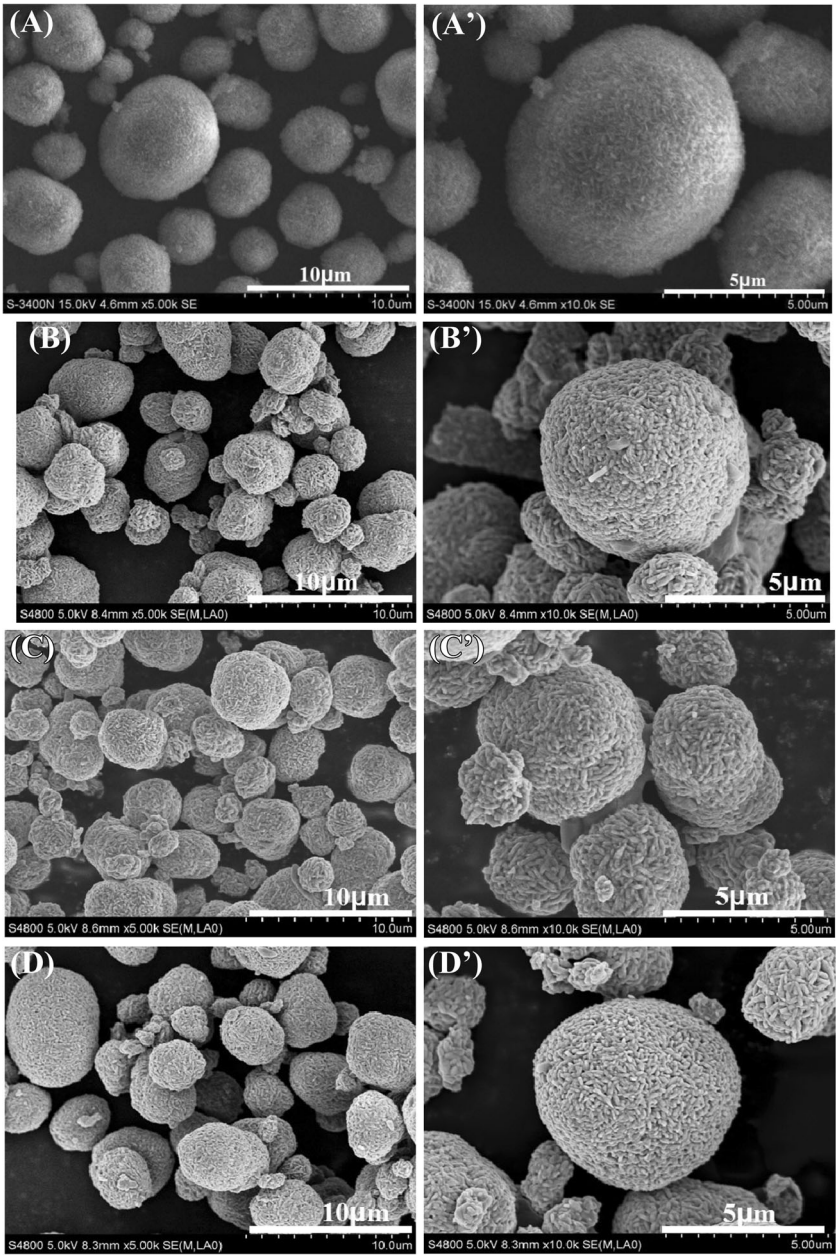

Fig. 2 SEM images of the $Ni_{0.8}Co_{0.15}(OH)_{1.9}$ precursor (*A* and *A′*) and $LiNi_{0.8}Co_{0.15}Ti_{0.05}O_2$ cathode materials prepared at different calcination temperature. (*B* and *B′*), (*C* and *C′*), and (*D* and *D′*) corresponded to NCT-1, NCT-2, and NCT-3 samples, respectively

an important influence on the electrochemical performance of $LiNi_{0.8}Co_{0.15}Ti_{0.05}O_2$ cathode materials. The $LiNi_{0.8}Co_{0.15}Ti_{0.05}O_2$ material prepared at a lower calcination temperature (750 °C) shows a poor electrochemical performance due to a lower degree of ordered layered structure hinders lithium-ion intercalation in charge/

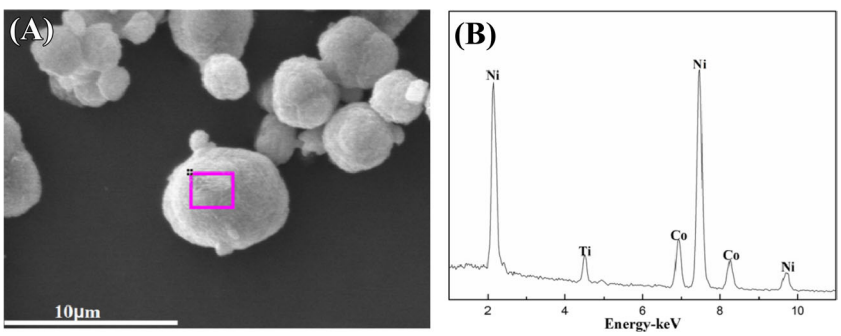

Fig. 3 SEM (**a**) and EDS (**b**) images of NCT-2 material

Table 2 The EDS analysis chart of the NCT-2 sample

Element	O	Ni	Co	Ti
Weight percentage (%)	44.07	45.19	8.65	2.08
Atomic percentage (%)	76.14	20.72	3.95	1.17

discharge process, which is consistent with XRD analysis results. This result shows that the lower temperature is insufficient to promote full lithium site ordering for nickel-rich-layered $LiNi_{0.8}Co_{0.15}Ti_{0.05}O_2$ cathode materials. Especially, the NCT-2 sample shows an excellent electrochemical performance attribute to higher degree of ordered layered structure and the least cation mixing [28]. The second crystallization phenomenon could be generated at a higher calcination temperature, which will also reduce the electrochemical performance. In addition, nonstoichiometry and disorder on the Li site will also be introduced due to the part volatilization of lithium at a higher temperature. The optimum temperature is required to synthesize the material with good crystallinity and stable layered structure. On the whole, all as-prepared $LiNi_{0.8}Co_{0.15}Ti_{0.05}O_2$ samples deliver smaller discharge specific capacity than typical values for commercial $LiNi_{0.8}Co_{0.15}Al_{0.05}O_2$ (190 mAh g^{-1}). To balance the valence electrons in this structure, the incorporated Ti^{4+} generated the same amount of Ni^{2+} by the principal of electroneutrality, resulting in the electrochemical inactivity of titanium should have a negligible contribution on the diminished capacities of $LiNi_{0.8}Co_{0.15}Ti_{0.05}O_2$ samples [29].

CV measurements were carried out in the voltage range of 2.5–4.5 V at a scan rate of 0.1 mV s^{-1} to further investigate the electrochemical reversibility of the $LiNi_{0.8}Co_{0.15}Ti_{0.05}O_2$ cathode materials. The CV curves of the first three cycles of NCT-1, NCT-2, and NCT-3 samples are shown in Fig. 5. Each of the three curves correspond to the first three charge/discharge process of the cathode material. There exist obvious differences about the CV curves of three samples, including the shape, current, and potential of peaks. Especially, the oxidation peak and the reduction peak of the NCT-2 sample shift toward low and high potential, respectively, resulting in a well-symmetry redox peak showed at approximate 3.8 V. In addition, the NCT-2 sample exhibits a sharper peak and a higher redox peak current than NCT-1 and NCT-3 samples. The results indicate that the NCT-2 sample reveals an advanced electrochemical reversibility and discharge

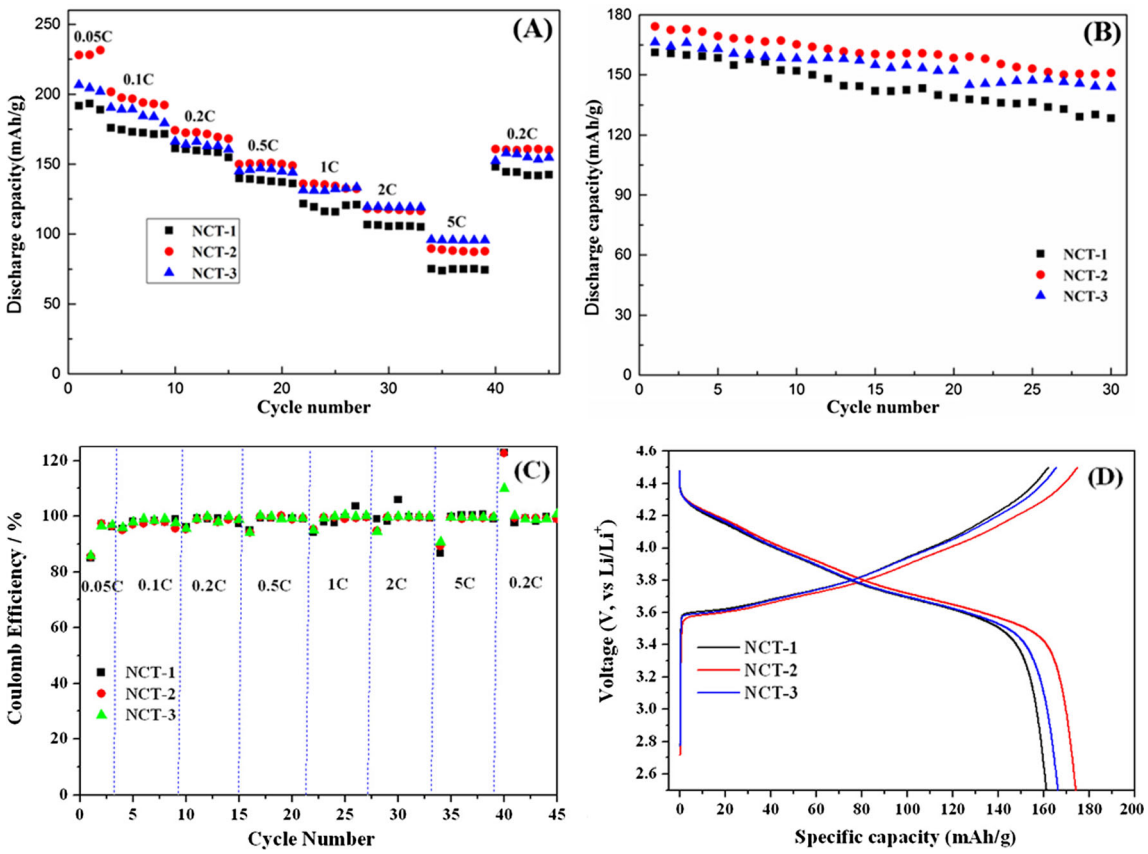

Fig. 4 The rate capability (**a**), cycling performance (**b**), Coulomb efficiency (**c**), and initial charge/discharge curves (**d**) of NCT-1, NCT-2, and NCT-3 samples, respectively

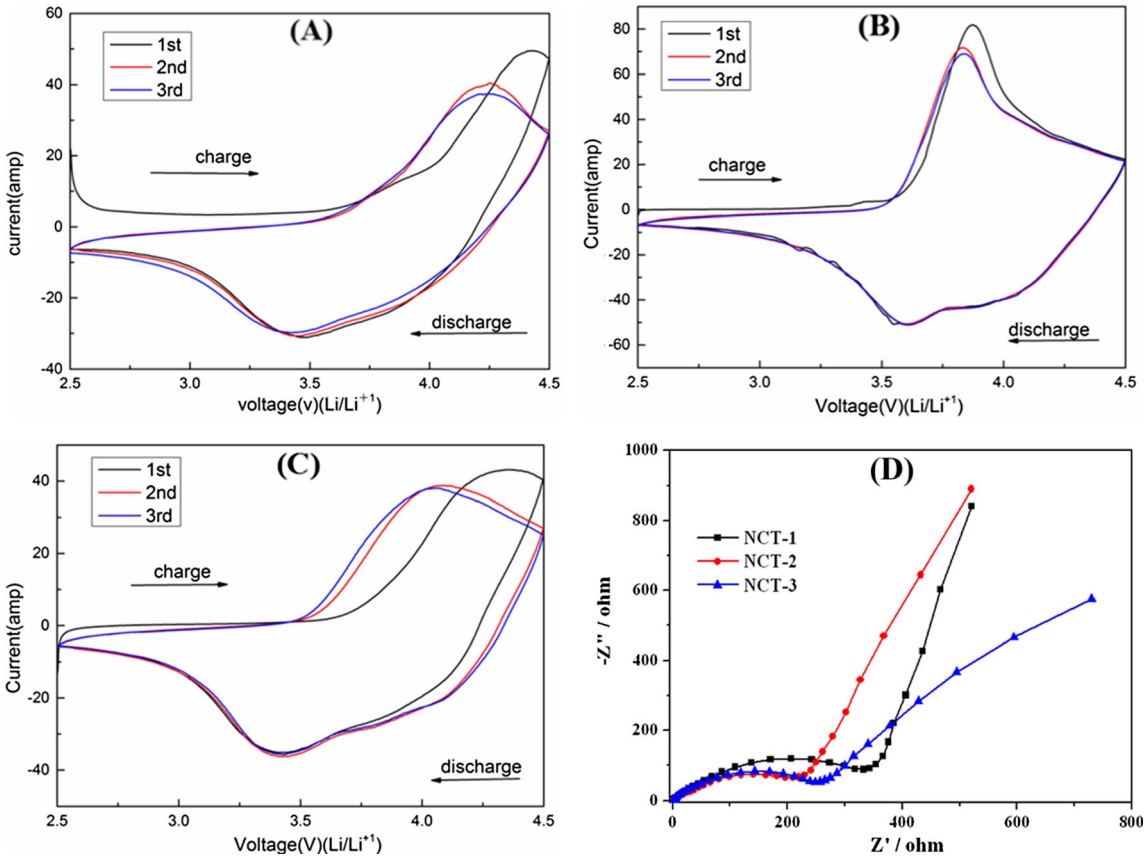

Fig. 5 Cyclic voltammograms of $LiNi_{0.8}Co_{0.15}Ti_{0.05}O_2$ cathode materials prepared at different calcination temperature. **a** NCT-1, **b** NCT-2, and **c** NCT-3 samples, respectively. **d** Nyquist plots of NCT-1, NCT-2, and NCT-3 samples

capacities. This conclusion is consistent with the previous analysis results from Fig. 4. The simplified CV curves and the peak shift are associated with the suppression of phase transitions due to superior maintenance of the layered structure after Ti addition. The improved stability of the layered structure is achieved by the presence of electrochemically inactive Ti^{4+} in the 3a site, which results better capacity retention during charge-discharge cycling [30].

In order to further understand the kinetic behavior of all as-prepared electrodes, EIS measurement was carried out using the half cells consisting of NCT-1, NCT-2, and NCT-3 samples as working electrode at the discharge state of 2.5 V after 30 cycles at 0.2 C. Figure 5d shows the Nyquist plots, which consist of two semicircles in high-to-medium frequency region and an inclined line in low frequency region for all samples [31]. Another semicircle at medium frequencies could be attributed to the charge-transfer resistance (R_{ct}). An intercept at the Zreal axis in the high-frequency region corresponds to the ohmic electrolyte resistance (R_e). The inclined line in the low-frequency region represents the Warburg impedance (Z_w), which is ascribed to the diffusion of the lithium ions in the bulk of electrode material. It is obviously observed that the ohmic electrolyte resistances are similar among the all electrodes. Especially, the R_{ct} (about 215 Ω cm^2) of NCT-2 sample is distinctly decreased compared with that of the NCT-1 (about 350 Ω cm^2) and NCT-3 (about 258 Ω cm^2) samples. This result indicates that Li ion migration at the surface of the NCT-2 cathode is significantly facilitated, ultimately resulting in an improved rate and cycle performance. This result is consistent with the rate and cycling performance in Fig. 4.

Conclusions

The spherical $LiNi_{0.8}Co_{0.15}Ti_{0.05}O_2$ cathode materials with a high tap density of 3.22 g cm^{-3} have been successfully prepared by using $Ni_{0.8}Co_{0.15}(OH)_{1.9}$ precursor. The electrochemical properties of $LiNi_{0.8}Co_{0.15}Ti_{0.05}O_2$ are greatly associated with the calcination temperature. The $LiNi_{0.8}Co_{0.15}Ti_{0.05}O_2$ sample prepared at 800 °C exhibits a higher degree of ordering hexagonal structure and the least cation mixing and reveals excellent electrochemical performance with the discharge capacity of 174.2 mAh g^{-1} and the capacity retention of 86.7 % after 30 cycles at 0.2 C.

References

1. Ito S, Fujiki S, Yamada T, Aihara Y, Park Y, Kim TY, Baek S-W, Lee J-M, Doo S, Machida N (2014) A rocking chair type all-solid-state lithium ion battery adopting Li_2O-ZrO_2 coated $LiNi_{0.8}Co_{0.15}Al_{0.05}O_2$ and a sulfide based electrolyte. J Power Sources 248:943–950
2. Park B-C, Kim H-B, Bang HJ, Prakash J, Sun Y-K (2008) Improvement of electrochemical performance of Li $[Ni_{0.8}Co_{0.15}Al_{0.05}]O_2$ cathode materials by AlF_3 coating at various temperatures. Ind Eng Chem Res 47:3876–3882
3. Cao D, Wu L, Sun Y (2008) Electrochemical behavior of Mg-Li, Mg-Li-Al and Mg-Li-Al-Ce in sodium chloride solution. J Power Sources 177:624–630
4. Wu SH, Su HJ (2003) Electrochemical characteristics of partially cobalt-substituted $LiMn_{2-y}Co_yO_4$spinels synthesized by Pechini process. Mater Chem Phys 78:189–195
5. Dompablo MEAY, Ceder G (2003) First-principles calculations on Li_xNiO_2: phase stability and monoclinic distortion. J Power Sources 119:654–657
6. Ohzuku T, Ueda A, Nagayama M (1993) Elctrochemistry and structural chemistry of $LiNiO_2$ (R3 over-bar-M) for 4 volt secondary lithium cells. J Electrochem Soc 140:1862–1870
7. Yoshio M, Noguchi H, Itoh J, Okada M (2000) Preparation and properties of $LiCo_yMn_xNi_{1-x-y}O_2$ as a cathode for lithium ion batteries. J Power Sources 90:176–181
8. Park TJ, Lim JB, Son JT (2014) Effect of calcination temperature of size controlled microstructure of $LiNi_{0.8}Co_{0.15}Al_{0.05}O_2$ cathode for rechargeable lithium battery. Bull Kor Chem Soc 35:357–364
9. Kim J, Amine K (2001) The effect of tetravalent titanium ubstitution in $LiNi_{1-x}Ti_xO_2$ ($0.025 \le x \le 0.2$) system. Electrochem Commun 3:52–55
10. Kim J, Amine K (2002) A comparative study on the substitution of divalent, trivalent and tetravalent metal ions in $LiNi_{1-x}M_xO_2$ ($M = Cu^{2+}$,Al^{3+}andTi^{4+}). J Power Sources 104:33–39
11. Myung ST, Komaba S, Hosoya K, Hirosaki N, Miura Y, Kumagai N (2005) Synthesis of $LiNi_{0.5}Mn_{0.5}$-xTi_xO_2 by an emulsion drying method and effect of Ti on structure and electrochemical properties. Chem Mater 17:2427–2435
12. Tang HW, Zhao FS, Chang ZR (2009) Synthesis and electrochemical properties of high density $LiNi_{0.8}Co_{0.2-x}Ti_xO_2$ for lithium-ion batteries. J Electrochem Soc 156:A478–A482
13. Liu GB, Liu H, Shi YF (2013) The synthesis and electrochemical properties of xLi_2MnO_3-(1-x)MO_2($M = Mn_{1/3}Ni_{1/3}Fe_{1/3}$) via co-precipitation method. Electrochim Acta 88:112–116
14. Zhu HL, Xie T, Chen ZY, Li LJ, Xu M, Wang WH, Lai YQ, Li J (2014) The impact of vanadium substitution on the structure and electrochemical performance of $LiNi_{0.5}Co_{0.2}Mn_{0.3}O_2$. Electrochim Acta 135:77–85
15. Xu Y, Li XH, Wang ZX, Guo HJ, Huang B (2015) Structure and electrochemical performance of TiO_2-coated $LiNi_{0.80}CO_{0.15}Al_{0.05}O_2$ cathode material. Mater Lett 143:151–154
16. Liu HS, Li J, Zhang ZR, Gong ZL, Yang Y (2004) Structural, electrochemical and thermal properties of $LiNi_{0.8-y}Ti_yCo_{0.2}O_2$ as cathode materials for lithium ion battery. ElectrochimicaActa 49: 1151–1159
17. Lin B, Wen ZY, Han J (2008) Electrochemical properties of carbon-coated $Li[Ni_{1/3}Co_{1/3}Mn_{1/3}]O_2$ cathode material for lithium-ion batteries. Solid State Ionics 179:1750–1753
18. Xiao LF, Yang YY, Zhao YQ (2008) Synthesis and electrochemical properties of submicron $LiNi_{0.8}Co_{0.2}O_2$ by a polymer-pyrolysis method. Electrochim. Acta 53:3007–3012
19. Yoon WS, Chung KY, McBreen J (2007) Electronic structural changes of the electrochemically Li-ion deintercalated $LiNi_{0.8}Co_{0.15}Al_{0.05}O_2$ cathode material investigated by X-ray absorption spectroscopy. J Power Sources 174:1015–1020
20. Kim Y, Yu D (2012) Synthesis of high-density nickel cobalt aluminum hydroxide by continuous coprecipitation method. ACS Appl Mater Interfaces 4:586–589
21. Guilmard M, Croguennec L, Denux D, Delmas C (2003) Thermal stability of lithium nickel oxide derivatives. Part I: $Li_xNi_{1.02}O_2$ and $Li_xNi_{0.89}Al_{0.16}O_2$ (x = 0.50 and 0.30). Chem Mater 15:4476–4483
22. Rougier A, Saadoune I, Gravereau P (1996) Effect of cobalt substitution on cationic distribution in $LiNi_{1-y}Co_yO_2$ electrode materials. Solid State Ionics 90:83–90
23. Mantuano DP, Dorella G, Elias RCA (2006) Analysis of a hydrometallurgical route to recover base metals from spent rechargeable batteries by liquid-liquid extraction with Cyanex 272. J Power Sources 159:1510–1518
24. Liu H, Stoll J, Henriksen M (2004) Aluminum-doped lithium nickel cobalt oxide electrodes for high-power lithium-ion batteries. J Power Sources 128:278–285
25. Gover RKB, Kanno R, Mitchell BJ, Yonemura M, Kawamoto Y (2000) Effects of sintering temperature on the structure of the layered phase $Li_x(Ni_{0.8}Co_{0.2})O_2$. J Electrochem Soc 147(11):4045–4051
26. Zhu XJ, Chen HH, Zhan H, Yang DL, Zhou YH (2004) Synthesis and characterization of $LiNi_{0.85}Co_{0.15-2x}(TiMg)_xO_2$ as cathode materials for lithium-ion batteries. Mater Chem Phys 88:145–149
27. Liu HS, Li J, Zhang ZR, Gong ZL, Yang Y (2003) The effects of sintering temperature and time on the structure and electrochemical performance of $LiNi_{0.8}Co_{0.2}O_2$ cathode materials derived from sol-gel method. J Solid State Electrochem 7:456–462
28. Hu GR, Liu WM, Peng ZD, Du K, Cao YB (2012) Synthesis and electrochemical properties of $LiNi_{0.8}Co_{0.15}Al_{0.05}O_2$ prepared from the precursor $Ni_{0.8}Co_{0.15}Al_{0.05}OOH$. J Power Sources 198:258–263
29. Dua R, Bi YJ, Yang WC, Peng Z, Liu M, Liu Y, Wu BM, Yang BC, Ding F, Wang DY (2015) Improved cyclicstability of $LiNi_{0.8}Co_{0.1}Mn_{0.1}O_2$ via Ti substitution with a cut-offpotential of 4.5 V. Ceram Int 41:7133–7139
30. Liu HS, Yang Y, Zhang JJ (2006) Investigation and improvement on the storage property of $LiNi_{0.8}Co_{0.2}O_2$ as a cathode material for lithium-ion batteries. J Power Sources 162:644–650
31. Cho Y, Cho J (2010) Significant improvement of $LiNi_{0.8}Co_{0.15}Al_{0.05}O_2$ cathodes at 60 °C by SiO_2 dry coating for Li-ion batteries. J Electrochem Soc 157:A625–A629